Journal of Alloys and Compounds 502 (2010) 176–179

Contents lists available at ScienceDirect

Journal of Alloys and Compounds

journal homepage: www.elsevier.com/locate/jallcom

Room-temperature ferromagnetism and ferroelectricity of nanocrystalline $La_2Ti_2O_7$

Li Sun, Jifan Hu*, Feng Gao, Xiangwei Kong, Hongwei Qin, Minhua Jiang

School of Physics, State Key Laboratory for Crystal Materials, Shandong University, Jinan 250100, People's Republic of China

ARTICLE INFO

Article history:
Received 21 January 2010
Received in revised form 10 April 2010
Accepted 23 April 2010
Available online 21 May 2010

Keywords:
Nanocrystalline
Multiferroic material
Ferromagnetism
Ferroelectricity

ABSTRACT

$La_2Ti_2O_7$ nanocrystalline powders and pellets were prepared by sol–gel method. The nanocrystalline powders present room-temperature ferromagnetism (FM). The vacuum annealing enhances FM, showing that the observed room-temperature FM for $La_2Ti_2O_7$ possibly originates from oxygen vacancies at/near surfaces of nanograins. $La_2Ti_2O_7$ pellets annealed at 1000 °C for 1 h show the coexistence of ferromagnetism and ferroelectricity (FE) at room temperature. Meanwhile, the room-temperature magnetodielectric (MD) effect was also observed in the $La_2Ti_2O_7$ multiferroic pellet, indicating the coupling between magnetic and electric properties. The value of $\Delta\varepsilon_r/\varepsilon_r(0)$ for $La_2Ti_2O_7$ multiferroic pellet reaches 39.3% at 1 kHz under H = 6 kOe.

1. Introduction

The multiferroic materials with coexistence of ferromagnetism (FM) and ferroelectricity (FE) are of particular interest since they present possibility for potential applications in spintronics, information storage and sensors [1]. Generally, most ferromagnetic oxides contain the center of symmetry and do not show electric polarization, while most sintered ferroelectric bulks are not magnetic [2]. However, more and more multiferroic materials were reported in recent years [3–13], e.g. $TbMnO_3$ [3,7], $BiFeO_3$ [5] and $BiMnO_3$ [6]. It can be expected that for the multiferroics with ferromagnetic and ferroelectric ordering simultaneously, the coupling between the magnetic and electric properties will lead to the magnetoelectric (ME) effect [1,3,5–7,9] in which the magnetization can be controlled by application of electric fields, and vice versa. The coupling can also give rise to the magnetodielectric (MD) [11,14] or magnetocapacitance (MC) effects [6,10], in which dielectric permittivity or capacitance can be adjusted by an applied magnetic field. Multiferroic composite materials consisting of both ferroelectric and ferromagnetic phases could yield giant magnetoelectric coupling response above room temperature, which are of potential applications [15,16].

Undoped oxides, such as HfO_2, TiO_2, Al_2O_3, In_2O_3, ZnO and MgO, have been found to exhibit weak FM at room temperature [17–24]. The observed FM may be related to the structural defects and size-confinement effects. Point defects in insulators might create localized electronic levels within the band gap, leading to different charge states and magnetic moments [25]. There were experimental evidences that the FM in HfO_2 and TiO_2 powders/films originated from oxygen vacancies [22,23]. However, an *ab initio* calculation demonstrated that cation vacancies were responsible for the magnetic moments in HfO_2 undoped oxide [26]. Both experimental and *ab initio* calculation [24,27] results showed that FM in nanocrystalline MgO originated from Mg vacancies at/near surfaces of nanograins.

Perovskite $BaTiO_3$ is a traditional ferroelectric material, and $BaTiO_3$ bulks sintered at high temperature are nonmagnetic. Recently, Mangalam et al. [28] reported the multiferroic properties with the coexistence of FM and FE in $BaTiO_3$ nanocrystalline (300 nm) pellet annealed at 1000 °C for 1 h. By first-principle calculation, they suggested that the FM of nanocrystalline $BaTiO_3$ might come from the oxygen vacancies and ferroelectricity from the core. A magnetocapacitance effect was observed in $BaTiO_3$ nanocrystalline (300 nm) pellet at room temperature [28]. $La_2Ti_2O_7$, which is a ferroelectric material with a high ferroelectric Curie temperature of 1500 °C [29,30], is a promising candidate for high-temperature piezoelectric and electro-optic devices [31–33]. Since the magnetic moments of both La atom and La^{3+} are zero and Ti element is nonmagnetic [34], there was no interest in the magnetism in bulk $La_2Ti_2O_7$ before. Whether the nanocrystalline $La_2Ti_2O_7$ is ferromagnetic or not? In this letter, we show that similar to undoped oxides HfO_2, TiO_2, Al_2O_3, In_2O_3, ZnO, MgO and $BaTiO_3$ [17–24,28], $La_2Ti_2O_7$ nanocrystalline powders present room-temperature FM. The vacuum annealing enhances FM, indicating that the FM in nanocrystalline $La_2Ti_2O_7$ possibly originates from oxygen vacancies at/near the surfaces of nanograins. The coexistence of FM

* Corresponding author. Tel.: +86 531 88377035; fax: +86 531 88377031.
E-mail address: hu-jf@vip.163.com (J. Hu).

0925-8388/$ – see front matter
doi:10.1016/j.jallcom.2010.04.137

Table 1
Different types of $La_2Ti_2O_7$ samples.

T_A (°C)	Annealing conditions		
700 (powders)	2 h in air	2 h in air + 20 min in vacuum	2 h in air + 20 min in vacuum + 20 min in air
800 (powders)	2 h in air		
1000 (powders)	2 h in air		
1000 (pellets)	30 min in air	1 h in air	1.5 h in air
1100 (pellet)	1 h in air		

and FE at room-temperature could be observed in $La_2Ti_2O_7$ pellets annealed at appropriate low temperatures and in proper time period. Meanwhile, the MD effect was also observed, which implied the coupling between FM and FE.

2. Experimental

$La_2Ti_2O_7$ powders were prepared by sol–gel method. 0.2 mol $La(NO_3)_3 \cdot 6H_2O$ with a purity of 99.99 wt% (without any ferromagnetic elements) and 0.2 mol tetra-n-butyl titanate with a purity of 99.99 wt% (without any ferromagnetic elements) were dissolved in 180 mL ethanol, with constant stirring at about 35 °C, to get the sol. The gel was obtained by stirring the sol at 65 °C for two days. The precursor was annealed at 700 °C, 800 °C and 1000 °C for 2 h in air, respectively. Parts of powders after annealing at 700 °C were reheated in vacuum at 700 °C for 20 min, and then parts of vacuum annealed powders were backfired in air at 700 °C for 20 min. Some $La_2Ti_2O_7$ powders were pressed with a mold (made from nylon), and then annealed at 1000 °C and 1100 °C, respectively. All the different types of $La_2Ti_2O_7$ samples are listed in Table 1. The structures of $La_2Ti_2O_7$ powders annealed at different temperatures were investigated by X-ray diffraction with Cu Kα radiation. The microstructure of the $La_2Ti_2O_7$ pellet annealed at 1000 °C for 1 h was observed by field emission scanning electron microscope (FE-SEM). The magnetic properties of all the samples were measured using alternating gradient magnetometer (AGM) at room-temperature. The ferroelectric properties of $La_2Ti_2O_7$ pellets were measured by a ferroelectric meter TF Analyzer 2000. The MD effect was measured with a HP 4294A impedance analyzer. Both surfaces of the $La_2Ti_2O_7$ pellets for ferroelectric and MD measurements were deposited with Ag.

3. Results and discussion

The X-ray diffraction patterns of $La_2Ti_2O_7$ as-synthesized powders are shown in Fig. 1. At 700 °C, $La_2Ti_2O_7$ powders are partly crystallized with an orthorhombic structure (group *Pna*21). The powders annealed above 800 °C crystallize with a monoclinic structure (group $P2_1$). Such phase transformation has been reported previously [35]. The average grain sizes of $La_2Ti_2O_7$ powders were estimated to be 28 nm for 700 °C and 33 nm for 800 °C by *Scherrer's* method.

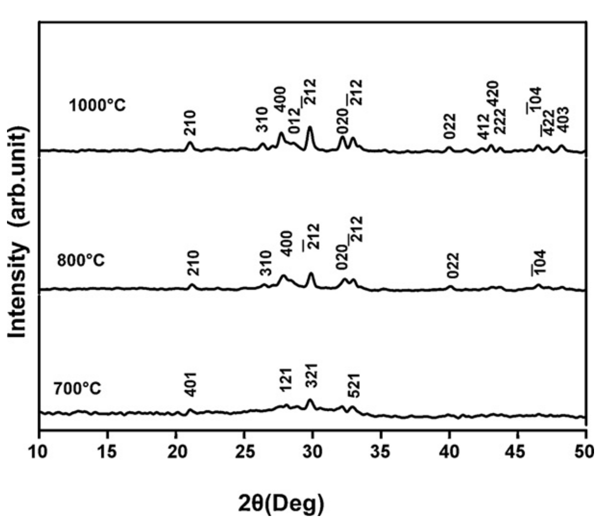

Fig. 1. The X-ray diffraction patterns of $La_2Ti_2O_7$ powders.

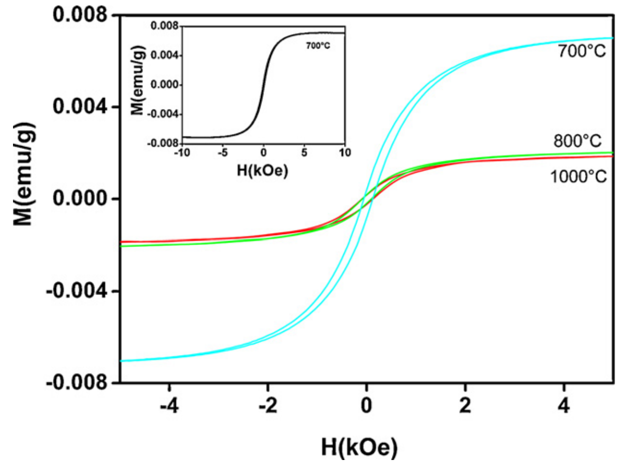

Fig. 2. The room-temperature *M–H* curves after DM corrections for $La_2Ti_2O_7$ powders with different annealing temperature from 700 to 1000 °C for 2 h. The inset is the room-temperature *M–H* curve (after DM correction) in a large field range for $La_2Ti_2O_7$ powders with T_A = 700 °C.

The magnetization (*M*) versus magnetic field (*H*) curves after diamagnetism (DM) correction for $La_2Ti_2O_7$ powders at room-temperature were shown in Fig. 2. $La_2Ti_2O_7$ nanocrystalline powders present hysteresis loops, showing room-temperature FM. The inset is the room-temperature *M–H* curve (after DM correction) in a large field range for $La_2Ti_2O_7$ powders with T_A = 700 °C. The values of *Ms* are 7.1×10^{-3} emu/g for T_A = 700 °C, 2.1×10^{-3} emu/g for T_A = 800 °C, and 1.9×10^{-3} emu/g for T_A = 1000 °C. In general, the room-temperature saturation magnetization *Ms* of oxide nanopowders, which contain no ferromagnetic element, is very small. For example, the value of *Ms* is $\sim 10^{-3}$ emu/g for $BaTiO_3$ [28]. The FM of $La_2Ti_2O_7$ nanocrystalline powders reduces with the increase of annealing temperatures T_A from 700 to 1000 °C, possibly due to the decrease of concentration of structural defects at/near the surfaces of grains.

Fig. 3 shows room-temperature *M–H* curves for $La_2Ti_2O_7$ powders annealed at 1000 °C (after DM correction), and pellets annealed at 1000 °C for 30 min (after DM correction), 1 h (after DM correction), 1.5 h (without DM correction) and 1100 °C for 1 h (without DM correction). The $La_2Ti_2O_7$ pellets annealed at T_A = 1000 °C for 30 min and 1 h also present room-temperature FM. A typi-

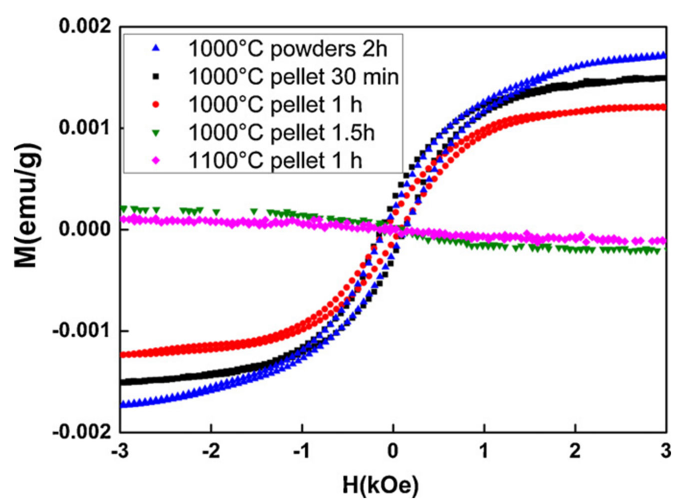

Fig. 3. The room-temperature *M–H* curves for $La_2Ti_2O_7$ powders annealed at 1000 °C (after DM correction), and pellets annealed at 1000 °C for 30 min (after DM correction), 1 h (after DM correction), 1.5 h (without DM correction) and 1100 °C for 1 h (without DM correction).

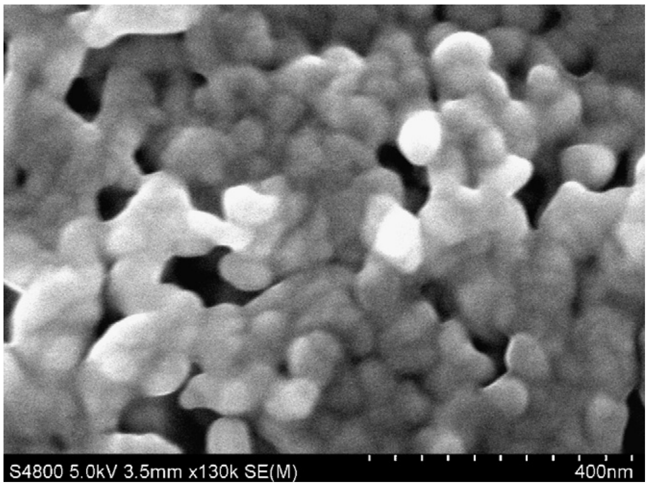

Fig. 4. The FE-SEM image of $La_2Ti_2O_7$ pellet annealed at 1000 °C for 1 h.

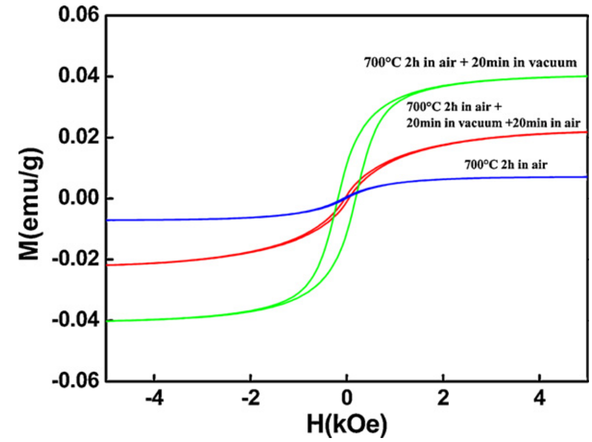

Fig. 5. The room temperature *M–H* curves after DM corrections for $La_2Ti_2O_7$ powders with different annealing conditions at 700 °C.

cal microstructure observed by a FE-SEM for the $La_2Ti_2O_7$ pellet annealed at 1000 °C for 1 h was shown in Fig. 4. The volume fraction of grains in this pellet is 15% for 20–50 nm grains, 19% for 50–100 nm grains, 66% for 100–225 nm grains. The average grain size of $La_2Ti_2O_7$ conventional bulks sintered at 1150 °C for 7 h was about 10–20 μm [32]. The magnetism of $La_2Ti_2O_7$ pellets depends sensitively on both annealing temperature and annealing time. $La_2Ti_2O_7$ pellets annealed at T_A = 1000 °C for 1.5 h and 1100 °C for 1 h exhibit diamagnetism (see Fig. 4). This is consistent with the fact that conventional $La_2Ti_2O_7$ sintered bulks are nonmagnetic. The values of *Ms* of $La_2Ti_2O_7$ pellets (T_A = 1000 °C for 30 min and 1 h) are lower than that of $La_2Ti_2O_7$ powders (T_A = 1000 °C for 2 h), due to the decrease of defect concentrations at the grain surfaces.

The observed FM in $La_2Ti_2O_7$ nanocrystalline powders does not originate from impurities, since the reactants do not contain any other ferromagnetic elements, and La/La^{3+}, as well as Ti, are nonmagnetic. Similar to the cases of undoped oxides HfO_2, TiO_2, Al_2O_3, In_2O_3, ZnO, MgO and $BaTiO_3$ [17–24,28], the observed FM in nanocrystalline $La_2Ti_2O_7$ should originate from structural defects. By first-principle calculation, Mangalam et al. suggested that the FM of nanocrystalline $BaTiO_3$ might come from the oxygen vacancies [28]. In order to experimentally verify whether FM originates from oxygen vacancies or cation vacancies, we have examined the influence of the vacuum annealing on magnetism of nanocrystalline $La_2Ti_2O_7$. Usually, the vacuum annealing effectively brings about some oxygen vacancies in semiconducting oxides. We found that after annealing at 700 °C in air, a subsequent annealing in vacuum at 700 °C for 20 min enhanced room-temperature FM of $La_2Ti_2O_7$ powders. The *Ms* value for the $La_2Ti_2O_7$ powders with the backfire in air after vacuum annealing is lower than that of the sample with vacuum annealing, but higher than that of the sample annealed at air (see Fig. 5). It shows that FM in $La_2Ti_2O_7$ powders mainly originates from oxygen vacancies. It was also reported that the FM of nanocrystalline HfO_2, TiO_2 and $BaTiO_3$ might come from the oxygen vacancies [21,23,28].

It is well known that $La_2Ti_2O_7$ sintered bulks present ferroelectric properties with a high ferroelectric Curie temperature and a high coercive field [29,30]. Usually, bulk materials with strong ferroelectric properties are prepared by sintering at high temperature. However, for $BaTiO_3$ [28] and $La_2Ti_2O_7$, FM properties disappear when the annealing temperature T_A is too high. In order to obtain the coexistence of FM and FE, the annealing temperature T_A should be carefully chosen. Fig. 6 shows the room-temperature polarization (*P*) versus electric field (*E*) curves for the $La_2Ti_2O_7$ pellet annealed at T_A = 1000 °C for 1 h. Hysteresis *P–E* loops were clearly observed for the $La_2Ti_2O_7$ pellet, showing the room-temperature FE. The *P–E* loops are not saturated, since the saturation electrical field is larger than what the equipment used here can provide.

The ferroelectric signal of the $La_2Ti_2O_7$ pellet annealing at T_A = 1000 °C for 1 h is weak and the loops are slim (see Fig. 6). These two phenomena are possibly connected with the low annealing temperature and the small applied electric field. The low annealing temperature with short annealing time leads to small-size grains. Many investigators have investigated grain-size effect on ferroelectric properties [36–39]. There is a reduction of FE with the decrease of grain size for ferroelectric nanomaterials. In addition, the *P–E* loops are not continuous (see Fig. 6) at the third and fourth quadrants. Similar *P–E* loops were also observed by other groups [9,28,40–42]. The shapes of *P–E* loops for our $La_2Ti_2O_7$ nanocrystalline pellet are very similar to those of *P–E* loops for multiferroics $Bi_{1-x}Ba_xFeO_3$ (x = 0.15) [9].

Our experimental results demonstrate that the $La_2Ti_2O_7$ nanocrystalline pellets annealed at T_A = 1000 °C for 1 h is a room-temperature multiferroic material with coexistence of FM and FE, even though both FM and FE are weak. The coexistence of FM and FE for $La_2Ti_2O_7$ pellets requires appropriate annealing temperature and time. Fig. 7 shows the AC electric field frequency dependence of dielectric constant (ε_r) measured at room-temperature (without DC magnetic field) for the $La_2Ti_2O_7$ pellet annealed at T_A = 1000 °C for 1 h. It is clear that the dielectric constant decreases with increasing frequency. This result can be explained by the phenomenon of dipole relaxation wherein at low frequencies the dipoles are able to follow the frequency of the applied field [9]. In order

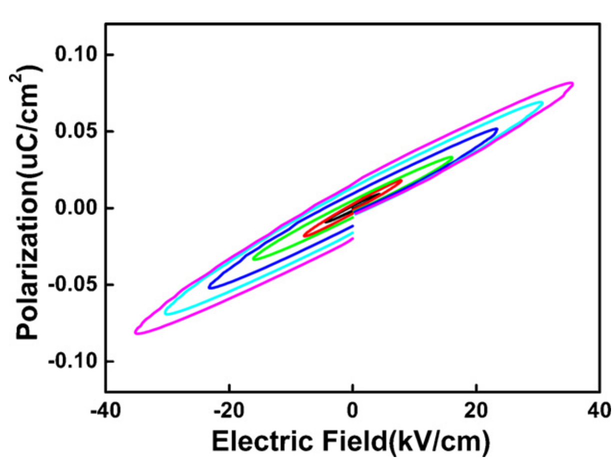

Fig. 6. *P–E* curves of $La_2Ti_2O_7$ pellet annealed at 1000 °C for 1 h.

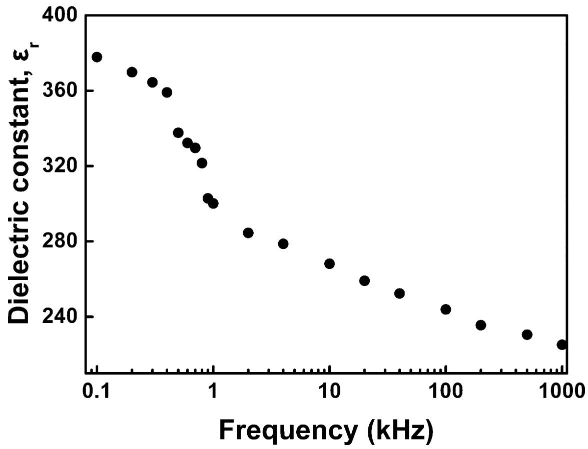

Fig. 7. Applied AC electric field frequency dependence of dielectric constant measured at room-temperature (without DC magnetic field) for $La_2Ti_2O_7$ pellet annealed at 1000 °C for 1 h.

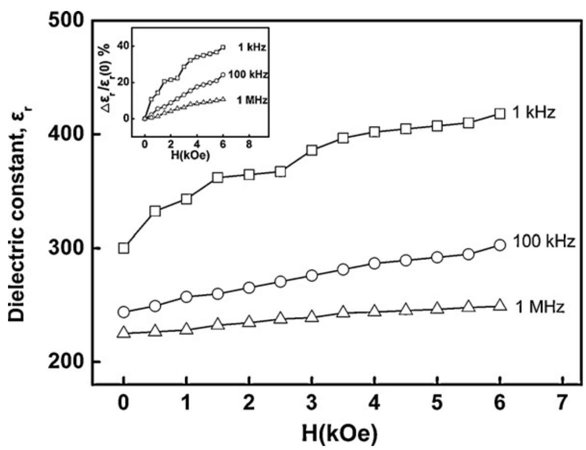

Fig. 8. Applied magnetic field dependence of dielectric constant measured at 1 kHz, 100 kHz and 1 MHz (at room temperature) for $La_2Ti_2O_7$ pellet annealed at 1000 °C for 1 h. The inset shows the magnetodielectric (MD) effect.

to test the coupling between electric and magnetic properties in the room-temperature multiferroic $La_2Ti_2O_7$ pellet, the applied magnetic field dependence of dielectric constant was measured at various frequencies (see Fig. 8). Room-temperature magnetodielectric effect was clearly observed. The field dependence of $\Delta\varepsilon/\varepsilon_r(0) = [\varepsilon_r(H) - \varepsilon_r(0)]/\varepsilon_r(0)$ for the $La_2Ti_2O_7$ pellet was also plotted in the inset of Fig. 8. With increasing magnetic field, the dielectric constant increases. Such results indicated that there is a coupling between magnetic and electric properties. As shown in the inset of Fig. 8, a positive MD effect occurs. The value of $\Delta\varepsilon_r/\varepsilon_r(0)$ reaches 39.3% at 1 kHz under $H = 6$ kOe. Positive magnetocapacitance (or magnetodielectric) effects were also observed in $BaTiO_3$ nanocrystalline pellets (annealed at 1000 °C for 1 h) [28] and $Bi_{1-x}Ba_xFeO_3$ compounds [9].

4. Conclusion

$La_2Ti_2O_7$ nanocrystalline powders prepared by sol–gel method present room-temperature FM. The FM of nanocrystalline powders may occur at the surface of nanograins. Vacuum annealing enhances FM of $La_2Ti_2O_7$ nanocrystalline powders. The observed FM in $La_2Ti_2O_7$ nanocrystalline powders may originate from oxygen vacancies at/near the surfaces of nanograins. $La_2Ti_2O_7$ pellets annealed at $T_A = 1000$ °C for 1 h present both room-temperature FM and FE. Meanwhile, $La_2Ti_2O_7$ multiferroic pellets also exhibit the room-temperature MD effect, indicating the coupling between magnetic and electric properties.

Acknowledgements

This work was mainly supported by National Natural Science Foundation of China (Nos.: 50872074 and 50872069). L. Sun and X.W. Kong acknowledge the support from National Found for Fostering Talents of Basic Science (No.: J0730318).

References

[1] N.A. Spaldin, M. Fiebig, Science 309 (2005) 391.
[2] N.A. Hill, J Phys. Chem. B 104 (2000) 6694.
[3] T. Kimura, T. Goto, H. Shintani, K. Ishizaka, T. Arima, Y. Tokura, Nature 426 (2003) 55.
[4] N. Hur, S. Park, P.A. Sharma, J.S. Ahn, S. Guha, S.-W. Cheong, Nature 429 (2004) 392.
[5] J. Wang, J.B. Neaton, H. Zheng, V. Nagarajan, S.B. Ogale, B. Liu, D. Viehland, V. Vaithyanathan, D.G. Schlom, U.V. Waghmare, N.A. Spaldin, K.M. Rabe, M. Wuttig, R. Ramesh, Science 299 (2003) 1719.
[6] T. Kimura, S. Kawamoto, I. Yamada, M. Azuma, M. Takano, Y. Tokura, Phys. Rev. B 67 (2003) 180401(R).
[7] N. Abe, K. Taniguchi, S. Ohtani, H. Umetsu, T. Arima, Phys. Rev. B 80 (2009) 020402(R).
[8] J. Wen, G. Xu, G. Gu, S.M. Shapiro, Phys. Rev. B 80 (2009) 020403(R).
[9] D.H. Wang, W.C. Goh, M. Ning, C.K. Ong, Appl. Phys. Lett. 88 (2006) 212907.
[10] M.P. Singh, W. Prellier, Ch. Simon, B. Raveau, Appl. Phys. Lett. 87 (2005) 022505.
[11] R. Ranjith, Asish K. Kundu, M. Filippi, B. Kundys, W. Prellier, B. Raveau, J. Laverdière, M.P. Singh, S. Jandl, Appl. Phys. Lett. 92 (2008) 062909.
[12] Q.H. Jiang, F.T. Liu, C.-W. Nan, Y.H. Lin, M.J. Reece, H.X. Yan, H.P. Ning, Z.J. Shen, Appl. Phys. Lett. 95 (2009) 012909.
[13] R. Seshadri, N.A. Hill, Chem. Mater. 13 (2001) 2892.
[14] N. Hur, S. Park, P.A. Sharma, S. Guha, S.-W. Cheong, Phys. Rev. Lett. 93 (2004) 017207.
[15] C.W. Nan, M.I. Bichurin, S.X. Dong, D. Viehland, G. Srinivasan, J. Appl. Phys. 103 (2008) 031101.
[16] H. Zheng, J. Wang, S.E. Lofland, Z. Ma, L. Mohaddes-Ardabili, T. Zhao, L. Salamanca-Riba, S.R. Shinde, S.B. Ogale, F. Bai, D. Viehland, Y. Jia, D.G. Schlom, M. Wuttig, A. Roytburd, R. Ramesh, Science 303 (2004) 661.
[17] M. Venkatesan, C.B. Fitzgerald, J.M.D. Coey, Nature 430 (2004) 630.
[18] N.H. Hong, J. Sakai, N. Poirot, V. Brizé, Phys. Rev. B 73 (2006) 132404.
[19] S.D. Yoon, Y. Chen, A. Yang, T.L. Goodrich, X. Zuo, K. Ziemer, C. Vittoria, V.G. Harris, J. Magn. Magn. Mater. 309 (2007) 171.
[20] A. Sundaresan, R. Bhargavi, N. Rangarajan, U. Siddesh, C.N.R. Rao, Phys. Rev. B 74 (2006) 161306.
[21] N.H. Hong, J. Sakai, N.T. Huong, N. Poirot, A. Ruyter, Phys. Rev. B 72 (2005) 045336.
[22] J.M.D. Coey, M. Venkatesan, P. Stamenov, C.B. Fitzgerald, L.S. Dorneles, Phys. Rev. B 72 (2005) 024450.
[23] N.H. Hong, J. Sakai, N.T. Huong, A. Ruyter, V. Brizé, Appl. Phys. Lett. 89 (2006) 252504.
[24] J.F. Hu, Z.L. Zhang, M. Zhao, H.W. Qin, M.H. Jiang, Appl. Phys. Lett. 93 (2008) 192503.
[25] A.M. Stoneham, Theory of Defects in Solids, Oxford University Press, Oxford, 1975.
[26] C.D. Penmaraju, S. Sanvito, Phys. Rev. Lett. 94 (2005) 217205.
[27] F. Gao, J.F. Hu, C.L. Yang, Y.J. Zheng, H.W. Qin, L. Sun, X.W. Kong, M.H. Jiang, Solid State Commun. 149 (2009) 855.
[28] R.V.K. Mangalam, Ray Nirat, Umesh V. Waghmare, A. Sundaresan, C.N.R. Rao, Solid State Commun. 149 (2009) 1.
[29] S. Nanamatsu, M. Kimura, K. Doi, S. Matsushita, N. Yamada, Ferroelectrics 8 (1974) 511.
[30] M. Kimura, S. Nanamatsu, T. Kawamura, S. Matsushita, Jpn. J. Appl. Phys. 13 (1974) 147.
[31] J.K. Yamamoto, A.S. Bhalla, J. Appl. Phys. 70 (1991) 4469.
[32] P.A. Fuierer, R.E. Newnham, J. Am. Ceram. Soc. 74 (1991) 2876.
[33] S. Marzullo, E.N. Bunting, J. Am. Ceram. Soc. 41 (1958) 40.
[34] H.R. Kirchmayr, C.A. Poldy, J. Magn. Magn. Mater. 8 (1978) 1.
[35] Z. Li, G. Chen, X. Tian, Y. Li, Mater. Res. Bull. 43 (2008) 1781.
[36] A.V. Bune, V.M. Fridkin, S. Ducharme, L.M. Blinov, S.P. Palto, A.V. Sorokin, S.G. Yudin, A. Zlatkin, Nature 391 (1998) 874.
[37] W.L. Zhong, B. Jiang, P.L. Zhang, J.M. Ma, H.M. Cheng, Z.H. Yang, L.X. Li, J. Phys. Condens. Matter 5 (1993) 2619.
[38] E.D. Mishina, K.A. Vorotilov, V.A. Vasiliev, A.S. Sigov, N. Ota, S. Nakabayashi, J. Exp. Theor. Phys. 122 (2002) 582.
[39] G. Geneste, E. Bousquet, J. Junquera, P. Ghosez, Appl. Phys. Lett. 88 (2006) 112906.
[40] J. Hao, Z. Xu, R. Chu, W. Li, G. Li, Q. Yin, J. Alloys Compd. 484 (2009) 233.
[41] J. Wu, J. Wang, J. Appl. Phys. 105 (2009) 124107.
[42] R. Font, O. Raymond, E. Martinez, J. Portelles, J.M. Siqueiros, J. Appl. Phys. 105 (2009) 114110.